

Design and Optimization of a Compact Inset Feed Microstrip Antenna for 5G Applications with Enhanced MIMO Performance

Jawdat S. Alkasassbeh

Electrical Engineering Department, Faculty of Engineering Technology, Al-Balqa Applied University, Amman, Jordan
Jawdat1983@bau.edu.jo (corresponding author)

Amjad Y. Hindi

Electrical Engineering Department, Faculty of Engineering Technology, Al-Balqa Applied University, Amman, Jordan
amjadhindi@bau.edu.jo

Issam Trrad

Computer Department, Jadara University, Irbid, Jordan
itrrad@jadara.edu.jo

Majed O. Dwairi

Electrical Engineering Department, Faculty of Engineering Technology, Al-Balqa Applied University, Amman, Jordan
majedd@bau.edu.jo

Elvira A. Dwairi

Electrical Engineering Department, Faculty of Engineering Technology, Al-Balqa Applied University, Amman, Jordan
alveradw@bau.edu.jo

Mahmoud Alja'fari

Al-Karak University College, Al-Balqa Applied University, Al-Karak, Jordan
Mzaj@bau.edu.jo

Received: 26 January 2025 | Revised: 26 January 2025 | Accepted: 6 February 2025

Licensed under a CC-BY 4.0 license | Copyright (c) by the authors | DOI: <https://doi.org/10.48084/etasr.10094>

ABSTRACT

This study presents the design, simulation, and optimization of a compact inset feed microstrip antenna for fifth-generation (5G) applications. With dimensions of $6.2 \times 8.4 \times 1.57 \text{ mm}^3$, the proposed antenna utilizes a Rogers RT5880 substrate ($\epsilon_r = 2.2$, loss tangent = 0.0013) and operates at resonant frequencies of 28 GHz and 26 GHz. The design, performed using CST Microwave Suite 2018, achieves an operational bandwidth of 5.368 GHz (25.144–30.512 GHz), with a relative bandwidth of 19.3%. At 28 GHz, the antenna exhibits a return loss of -25.166 dB and a gain of 7.33 dB, while at 26 GHz, it achieves a return loss of -13.2 dB and a gain of 7.88 dB. Enhancements using a 2-by-1 MIMO configuration, including inverted, mirrored, and nearby arrangements, were investigated. The inverted configuration demonstrated the highest gains of 8.15 dB and 7.96 dB at 26 and 28 GHz, respectively. The proposed antenna demonstrates applicability in compact mobile devices, Internet of Things (IoT) systems, and smart city infrastructure, underlining its practical relevance.

Keywords-microstrip antenna; 5G applications; MIMO configuration; bandwidth optimization; CST microwave suite

I. INTRODUCTION

The advent of 5G communication technology has revolutionized telecommunications by significantly enhancing data rates and capacity within the millimeter-wave spectrum. This advancement facilitates communication speeds over 100 times faster than fourth-generation (4G) systems, promoting applications, such as mobile communication, artificial intelligence, smart city connectivity, GPS, RFID, blockchain, and IoT. However, designing antennas compatible with high-frequency 5G bands, poses challenges in achieving compactness, high gain, and wide bandwidth [1-3].

Microstrip antennas have emerged as a leading solution due to their lightweight, low-cost, and easy-to-fabricate characteristics. Previous studies have demonstrated gains ranging from 5.06 to 12.7 dB for rectangular and arrayed microstrip patch antennas. Despite these advancements, the need for compact designs with improved gain and operational bandwidth remains unmet [4-6]. This study addresses the gap in achieving compact designs with high gain and wide bandwidth. While previous works have achieved gains ranging from 5.06 to 12.7 dB, the need for optimized designs persists. The proposed antenna achieves notable improvements in gain and operational bandwidth, tailored for 5G applications at 28 GHz and 26 GHz. Key practical uses include integration into smartphones, IoT devices, and other compact systems.

More complex antenna designs have been explored for wideband reception, covering multiple resonant frequencies with gains ranging from 5.7 to 9.21 dB [7-9]. For instance, an antenna array modification resulting in a gain of 12.7 dB was proposed [10]. Additionally, a two-element microstrip antenna operating at 28 and 38 GHz yielded gains of 7.51 and 9.712 dB, respectively, was presented in [11]. Even, designing L-slotted antennas with super high gains can achieve 11.26 dBi at 28.2 GHz [12]. Additionally, multiband antennas can operate at 28 GHz and 38 GHz with gains of 6.7 dB and 7.92 dB, respectively [13]. A wideband antenna covering 25–40 GHz reported gains of 7.18 to 7.2 dB [14], while microstrip antennas operating at 29.6 GHz and 28 and 50 GHz achieved gains of 5.51 dB and 2.6 dB, respectively [15-16]. Numerous studies have also explored ultra-wideband and MIMO microstrip patch antennas to enhance bandwidth and increase gain [17-22].

The main goal of this study is to develop an inset feed microstrip antenna that operates at a resonant frequency of 28 GHz and provides substantial gain. Furthermore, the study aims to enhance the received signal without increasing the transmitted power by utilizing various 2-by-1 MIMO antenna configurations.

II. ANTENNA DESIGN PARAMETERS

The proposed antenna operates at 28 GHz, a frequency chosen for its advantages, including minimal interference, short wavelength, and support for high data rate applications. The Rogers RT5880 substrate, with a permittivity (ϵ_r) of 2.2, was selected due to its low loss tangent and excellent thermal stability. Key design parameters, such as substrate height and feed line dimensions, were optimized using CST Microwave Suite 2018 because of its fast time-domain solver, intuitive

interface, efficient meshing, multi-physics integration, and superior performance in broadband antenna and PCB simulations over HFSS and other tools.

To enhance performance, elliptical extensions were incorporated into the patch antenna design, and the inset feed gap was matched to 50Ω to ensure maximum power transfer. The optimized antenna dimensions are presented in Table I.

TABLE I. THE PROPOSED ANTENNA PARAMETERS CALCULATED AND OPTIMIZED

Parameters	Calculated mm	Optimized mm
W_s	13.65	8.4
L_s	11.88	6.2
W_p	4.23	3.56
L_p	2.46	3.14
h_s	≤ 3.45	1.57
$t_p=t_g$	0.05	0.05
L_f	4.71	2.51
W_g	13.65	8.4
L_g	11.88	6.2
R_0		2
Inset feed gap	V_0	0.64
	X_0	0.42
r_0 (semi minor axis)		0.35

The antenna design is based on the operating frequency (f), the substrate height (h_s), and the ϵ_r . All parameters (Table I) are established and well-documented in [23–25], and calculated by:

$$h_s \leq \frac{0.3c}{2\pi f \sqrt{\epsilon_r}} \leq \frac{0.3 \cdot 3 \cdot 10^8}{2\pi \cdot 28 \cdot 10^9 \sqrt{2.2}} \leq 3.45 \quad (1)$$

$$W_p = \frac{c}{2f_r} \sqrt{\frac{2}{\epsilon_r + 1}} \quad (2)$$

$$\epsilon_{reff} = \frac{\epsilon_r + 2}{2} + \frac{\epsilon_r - 1}{2 \sqrt{1 + 12 \frac{h_s}{W_p}}} \quad (3)$$

$$\Delta L = \frac{0.412 \cdot h_s (\epsilon_{reff} + 0.3) \left(\frac{W_p}{h_s} + 0.264 \right)}{(\epsilon_{reff} - 0.258) \left(\frac{W_p}{h_s} + 0.8 \right)} \quad (4)$$

$$L_p = L_e - 2\Delta L \quad (5)$$

$$L_s = L_p + 6h_s \quad (6)$$

$$W_s = W_p + 6h_s \quad (7)$$

To ensure the maximum power transfer from the feed line to the antenna, the inset feed gap is selected to be matched with 50Ω , where the antenna is connected. The inset feed gap (f_{gap}) has a value of 2 mm and is calculated by:

$$f_{gap} = \frac{4.65 \cdot 10^{-18} \cdot c \cdot f_r}{\sqrt{2\epsilon_{reff}}} \quad (8)$$

To determine the dimensions of the feed line, the auxiliary variables a and b , for $Z_c = 50 \Omega$ were calculated by (9), (10) and have values $a=1.158$ and $b=7.97$:

$$a = \frac{Z_c}{60} \sqrt{\frac{\epsilon_r}{2} + \frac{\epsilon_r - 1}{\epsilon_r + 1} \left(0.23 + \frac{0.11}{\epsilon_r} \right)} \quad (9)$$

$$b = \frac{60\pi^2}{Z_c \sqrt{\epsilon_r}} \quad (10)$$

The width and length of the feed line were calculated using:

$$W_f = \frac{2}{\pi} \left\{ b - 1 - \ln(2b - 1) + \frac{\epsilon_r - 1}{2\epsilon_r} \cdot \left[\ln(b - 1) + 0.39 - \frac{61}{\epsilon_r} \right] \right\} \quad (11)$$

$$L_f = 3 \cdot h_s \quad (12)$$

The selection of 28 GHz as the operating frequency was driven by several factors. This frequency band offers multiple bandwidths, critical for supporting high data rates and accommodating multiple users. Additionally, its short wavelength enables compact antenna designs and high-speed performance in short-range communication systems. The relatively low interference levels at this frequency further enhance its suitability for the proposed design.

The ground plane of the patch antenna is designed to have the same dimensions as the substrate. To enhance the antenna's performance for resonance at 28 GHz, additional elliptical extensions were added to both sides of the patch antenna, allowing for adjustments in its dimensions to achieve the desired resonance. The semi-major axis of these extensions matches the patch length. The fully optimized antenna design is depicted in Figure 1.

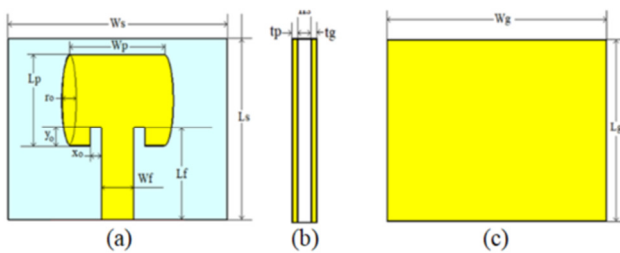


Fig. 1. The proposed microstrip antenna with inset feed: (a) visible view, (b) side view, (c) rear view.

III. THE PROPOSED ANTENNA RESULTS

The proposed 5G antenna, was designed, analyzed, and simulated using CST STUDIO SUITE 2018, with the substrate chosen being Rogers RT5880, with a permittivity of 2.2 mm and a height of 1.57 mm. The resonant frequency of the

antenna is 28 GHz with a reflection coefficient $S_{11} = -25.166$, as portrayed in Figure 2. The bandwidth ($S_{11} \leq -10$ dB) ranges from 25.144 GHz to 30.512 GHz, which means that the operating bandwidth is 5.398 GHz.

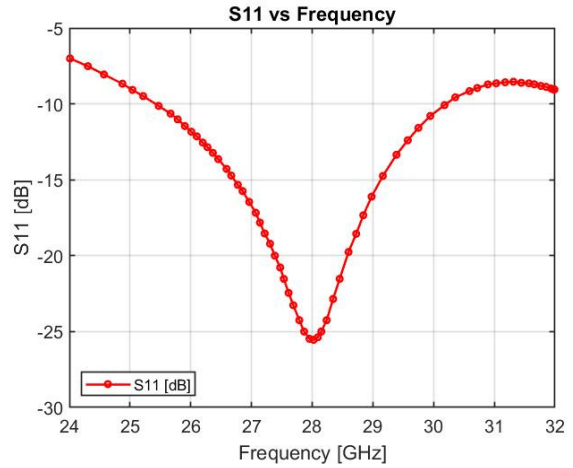


Fig. 2. Simulation results of the proposed 5G inset feed microstrip antenna.

The gain of the proposed antenna varies over the operating bandwidth from 5.42 to 7.69 dB, with 7.38 dB at 28 GHz, as shown in Figure 3, and is sufficient for 5G antenna applications.

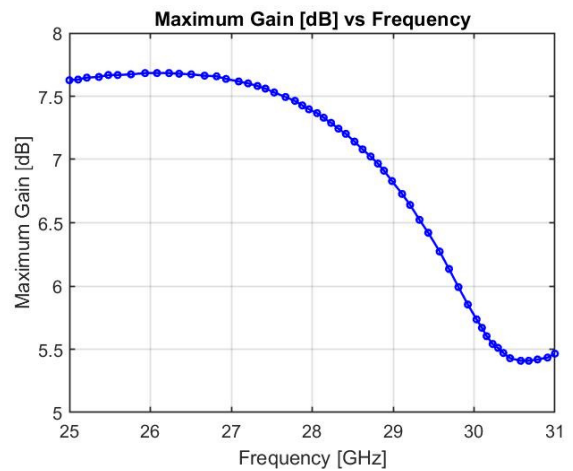


Fig. 3. The released gain of the proposed 5G inset feed microstrip antenna.

The 2D radiation patterns for the proposed antenna at resonant frequencies of 26, and 28 GHz are illustrated in Figure 4. It seems that the antenna is directional, with a gain of 7.3 dBi for the main lobe and -17.9 and -18.2 dB for the side lobes, which is much less than the threshold value of -13.46 dB, while the Half-Power Beam Width (HPBW) ranges from 82.3° to 90.9°, respectively.

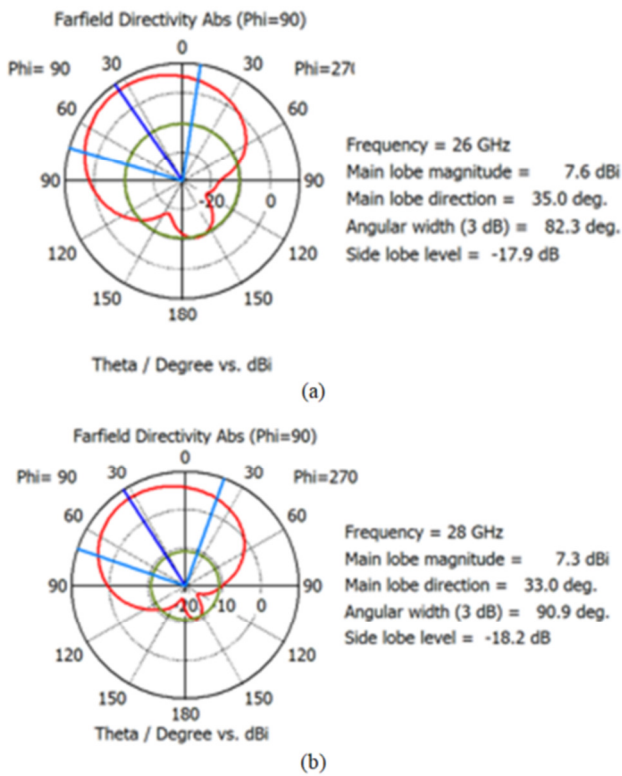


Fig. 4. 2D radiation patterns for (a) 26 GHz, (b) 28 GHz.

IV. MIMO ANTENNAS DESIGN

Many related works have deployed MIMO antennas, whether they were 2-by-1 or 2-by-2 [20–22], to increase the realized gain. Authors in [20] modified an antenna to a 2-by-1 MIMO antenna, receiving about a 1.5 dB increase in the realized gain, while authors in [21] investigated the effect of changing the formation of the 2-by-1 and 2-by-2 antennas in MIMO antennas on the realized gain by testing many formations of MIMO antennas and analyzing the results to choose the best-realized gain. Authors in [22] evaluated different antenna modifications and obtained an increased gain ranging from 1 to 2.5 dB. In the present study, the initial antenna was modified in a 2-by-1 MIMO antenna to evaluate its ability to increase gain [20–22]. Three MIMO configurations (nearby, inverted, and mirrored) were studied as they have shown good results in previous studies.

A. Nearby Orientation

The proposed 2-by-1 MIMO antenna with a nearby configuration, as can be seen in Figure 5, comprises two antennas which are etched in the substrate nearby with the same dimensions as those of the original antenna. Also, the substrate length is the same as that of the original antenna, while the substrate width is twice that of the original single antenna, with an additional width R_o separating the ground of the nearby antennas to minimize the mutual effects.

The simulated results of the return loss, as evidenced in Figure 6, of the two antennas S_{11} , S_{22} and the mutual return loss of S_{12} and S_{21} , show that the antenna has a resonant at 28 GHz

with a return loss of about -24.3 dB for both antennas, and the operating bandwidth is from 25.3 to 30.77 GHz, giving a bandwidth of 5.47 GHz.

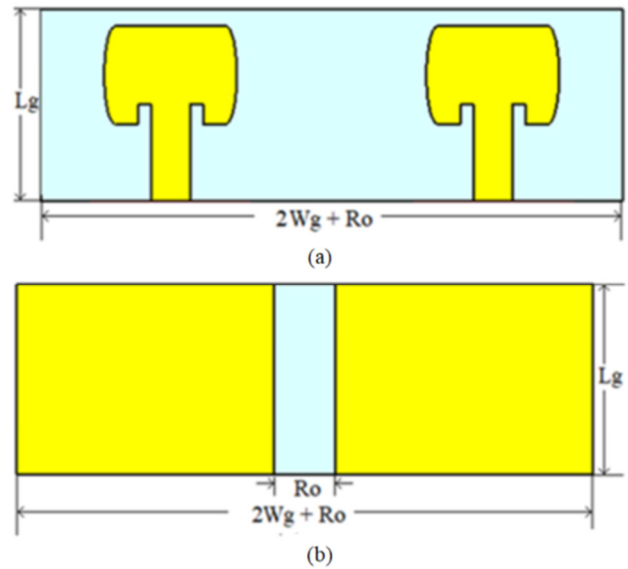


Fig. 5. (a) The proposed 2-by-1 MIMO antenna, (b) the ground of MIMO antenna.

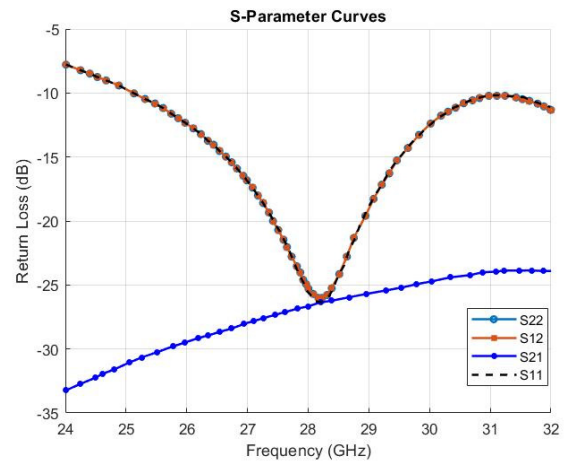


Fig. 6. Simulated S_{11} , S_{22} , and the coupling S_{12} and S_{21} for the 2-by-1 nearby MIMO antenna.

Figure 7 depicts the simulated realized gain for the neighboring MIMO antenna across the frequency range (24 GHz to 32 GHz). The gain varies over the bandwidth from 5.7 to 7.96 dB. The realized gain at 28 GHz is 7.58 dB, about 0.18 dB more than in the single antenna.

In the nearby configuration, two antennas were etched on the same substrate with minimal separation to reduce mutual coupling. This configuration achieved a return loss of -24.3 dB and a bandwidth of 5.47 GHz, with a maximum gain of 7.96 dB at 26 GHz.

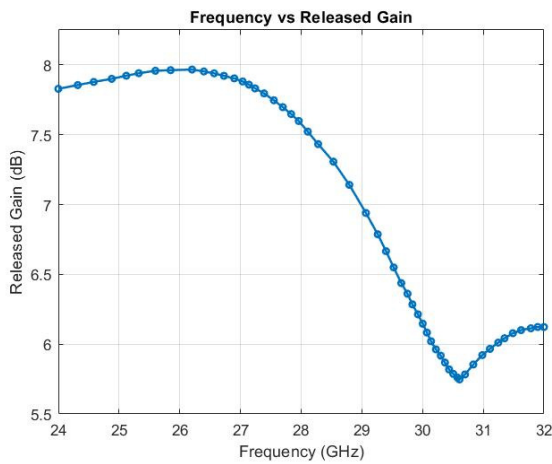


Fig. 7. Simulated realized gain for the neighboring MIMO antenna across the frequency range (24 to 32 GHz).

B. Inverted Orientation

In the proposed 2-by-1 inverted MIMO antenna, as displayed in Figure 8, the length of the substrate is the same as the length of the single element, while the width of the substrate is the same as that of the nearby MIMO for the same reasons. Both antennas are identical with one of them being inverted upside down.

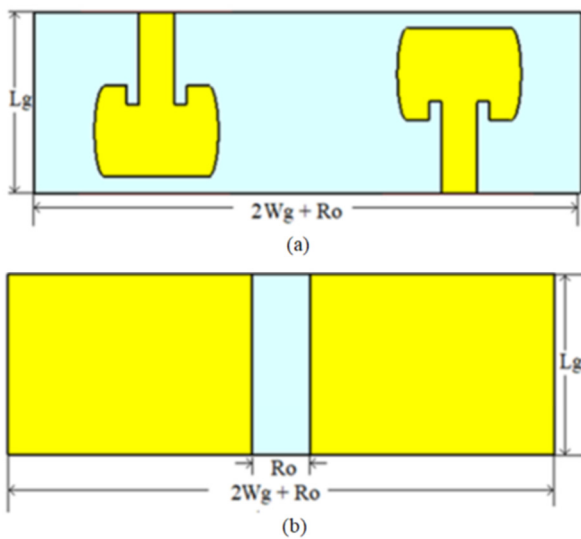


Fig. 8. (a) The proposed 2-by-1 inverted MIMO antenna, (b) the ground of the MIMO antenna.

The simulation results of the return loss, as portrayed in Figure 9, show that the reflection coefficient at 28GHz is -25.84 dB and the operating bandwidth ranges from 25.28 to 30.63 GHz, with a bandwidth of 5.35 GHz, which is a little less than that of the nearby MIMO antenna.

The realized gain varies over the operated bandwidth from 5.7 to 8.16 dB. The gain at 28 GHz is 7.63 dB, which is by 0.42 dB more than that of the single antenna. The maximum gain achieved at 26 GHz is 8.16 dB, as can be seen in Figure 10.

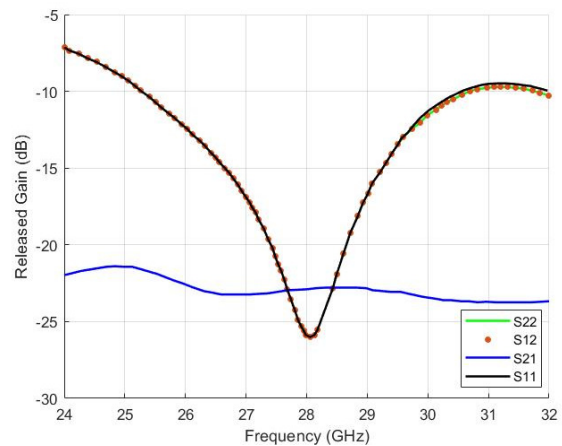


Fig. 9. Simulated S_{11} , S_{22} , and the coupling S_{12} and S_{21} for the 2-by-1 inverted MIMO antenna.

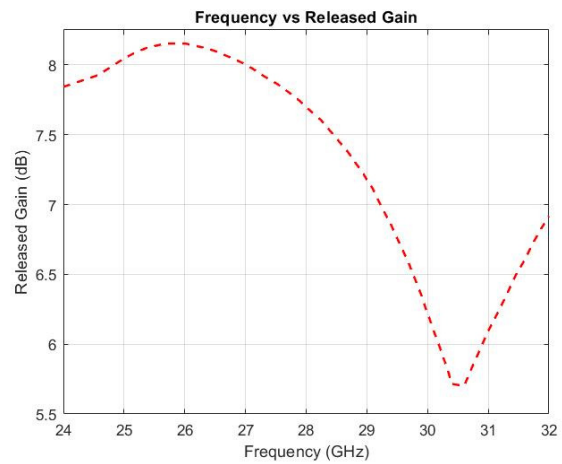


Fig. 10. Simulated realized gain for the 2-by-1 inverted MIMO antenna.

The inverted configuration featured one antenna flipped upside down. This setup resulted in the highest gain of all configurations, reaching 8.16 dB at 26 GHz and 7.63 dB at 28 GHz. The bandwidth was slightly lower than the nearby arrangement, measuring 5.35 GHz.

C. Mirrored Orientation

The proposed 2-by-1 mirrored MIMO antenna is configured by doubling the length of the single antenna design substrate and adding R_o , to avoid coupling interference between the proposed antennas, as illustrated in Figure 11. The return loss of both antennas is identical, as depicted in Figure 12. The coupling return loss of both antennas is identical as well. The resonant frequency has become a little less than 28 GHz, which is about 27.8 GHz, while the operating band ranges from 24 to 30.35 GHz, with an operating bandwidth of 6.35 GHz, which is more than the bandwidth of a single antenna, nearby MIMO, and inverted MIMO by 0.952, 0.88, and 1 GHz, respectively. The simulated realized gain for the proposed antenna, as evidenced in Figure 13, demonstrates that the realized gain in the operational bandwidth ranges from 6.7 to 7.73 dB, with the highest gain having been recorded at 27.5 GHz.

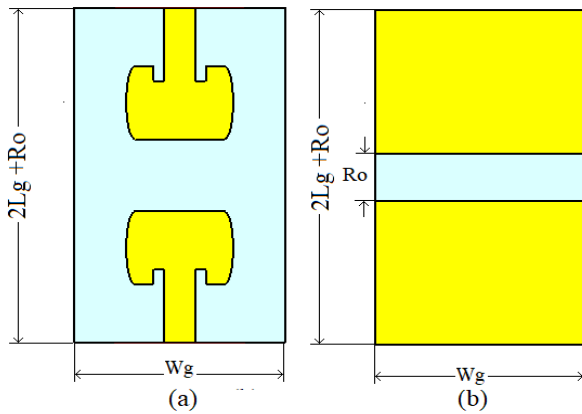


Fig. 11. (a) The proposed 2-by-1 mirrored MIMO antenna, (b) the ground of the MIMO antenna.

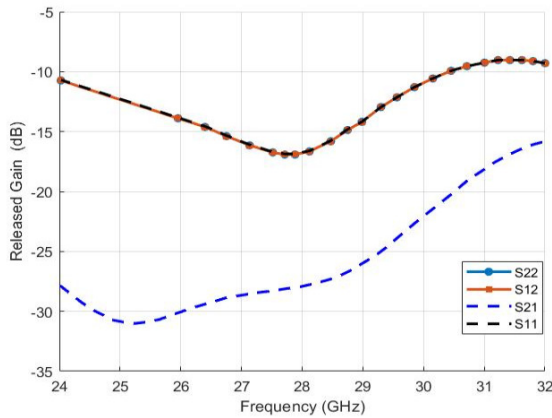


Fig. 12. Simulated S_{11} , S_{22} , and the coupling S_{12} and S_{21} for the 2-by-1 mirrored MIMO antenna.

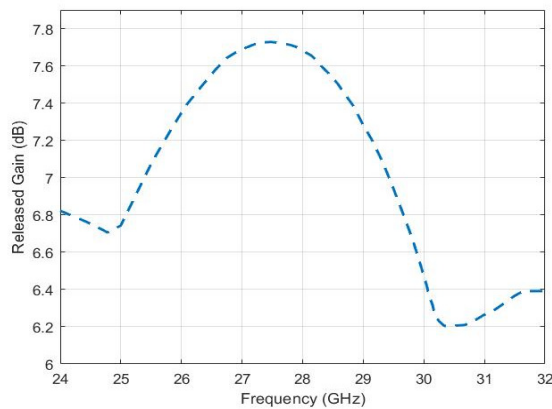


Fig. 13. Simulated realized gain for the 2-by-1 mirrored MIMO antenna.

V. RESULTS AND DISCUSSION

This study presented various 5G antenna designs operating around the 28 GHz frequency. The results confirm that the proposed antenna effectively operates at the desired 28 GHz resonant frequency, achieving an enhanced operational bandwidth of 5.398 GHz (25.144–30.512 GHz) and a realized gain of 7.4 dB at resonance. Across the operational bandwidth,

the gain ranged from 5.42 to 7.64 dB. Figure 14 provides a comparative analysis of the single antenna and all proposed 2-by-1 MIMO configurations.

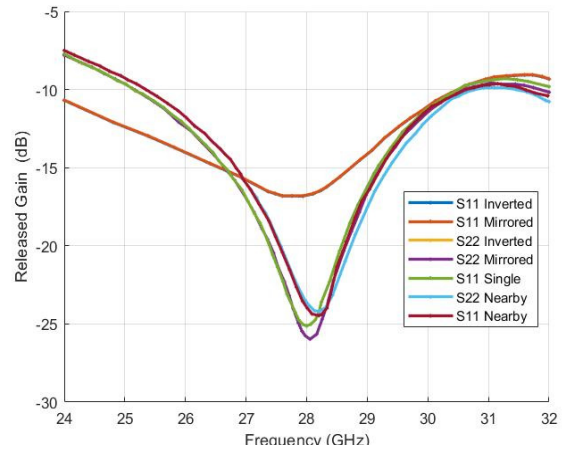


Fig. 14. Comparison of the return loss of the single antenna with the proposed MIMO antennas.

The 2-by-1 inverted MIMO antenna exhibits the most comparable to the single antenna performance metrics. Notably, the flipped antenna configuration achieved approximately 1 GHz wider bandwidth than the single antenna and other MIMO configurations, highlighting its potential for broader applications, as outlined in Table II.

TABLE II. COMPARATIVE FINDINGS BETWEEN THE SINGLE ANTENNA AND THE PROPOSED MIMO ANTENNAS

Investigated antennas	Resonant frequency [GHz]	Return loss at resonant [dB]	Operated BW [GHz]	BW [GHz]
Single	28	-25.2	25.144 - 30.512	5.37
Nearby	S11	28.17	25.3 - 30.77	5.47
	S22	28.18		
Inverted	S11	28.07	25.28 - 30.63	5.35
	S22	28.07		
Mirrored	S11	27.8	24 - 30.35	6.35
	S11	27.8		

The selection of nearby, inverted, and mirrored MIMO configurations was based on their potential to enhance gain and bandwidth while addressing mutual coupling. The mirrored configuration’s wider bandwidth (6.35 GHz) highlights its suitability for broader applications. Mutual Coupling mitigation techniques, such as separating antenna grounds and flipping orientations, minimize coupling. For example, the inverted MIMO achieves a coupling loss of -25.84 dB, reducing interference. It is observed that the gain across the operating bandwidth (BW) for all MIMO antennas is higher than that of a single antenna. At the resonant frequency, the gain is improved by 0.1 dB, 0.25 dB, and 0.34 dB for the nearby, inverted, and mirrored configurations, respectively, compared to the single antenna. Notably, the gain at 26 GHz is superior to that at the resonant frequency of 28 GHz for the single, nearby, and inverted MIMO configurations, as observed in Figure 15 and Table III. This indicates that the proposed antenna is well-suited for 5G applications at 26 GHz.

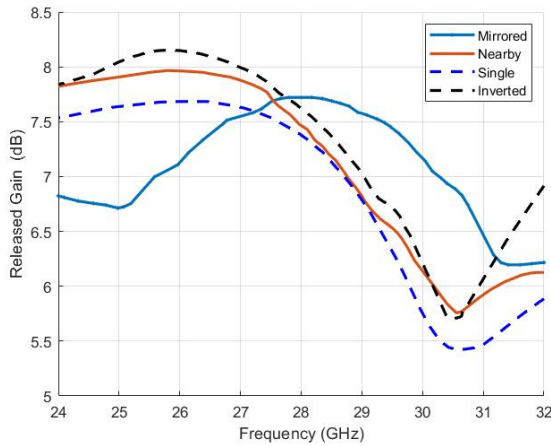


Fig. 15. Simulated realized gain for the single antenna and all proposed 2-by-1 MIMO antennas.

The single antenna achieved a return loss of -25.2 dB and a released gain of 7.38 dB at 28 GHz. The 2-by-1 MIMO configurations demonstrated enhanced performance, with gains ranging from 7.96 dB to 8.16 dB and operational bandwidths extending to 6.35 GHz.

The proposed antenna designs offer several notable benefits over existing works. Their compact size enabled by the use of

Rogers RT5880 substrate, addresses space constraints in 5G devices while maintaining high performance in addition to 6G frequencies [26]. The enhanced gain and bandwidth across both single and MIMO configurations ensure efficient signal transmission and wide coverage [27]. Compared to other studies, the proposed designs demonstrate clear advantages, such as higher relative bandwidth, competitive gain, and smaller size. These positive attributes position the proposed designs as highly effective solutions for 5G applications, including mobile devices, IoT systems, and smart city infrastructure, while providing a robust foundation for future advancements in wireless communication technology. The comparative analysis in Table IV highlights key trade-offs among gain, size, and bandwidth in the proposed designs and previous works.

TABLE III. COMPARATIVE ANALYSIS OF REALIZED GAIN FOR THE SINGLE ANTENNA AND THE PROPOSED MIMO CONFIGURATIONS

Investigated antennas	Maximum gain [dB]	Operated BW gain [dB]	Gain at resonant frequency [dB]
Single	7.69 at 26 GHz	5.42-7.69	7.38
Nearby	7.96 at 26 GHz	5.7- 7.96	7.48
Inverted	8.16 at 26 GHz	5.7- 8.16	7.63
Mirrored	7.72 at 28 GHz	6.7- 7.73	7.72

TABLE IV. COMPARISON BETWEEN CURRENT WORK AND OTHER REPORTED WORKS

Reference	Antenna size [mm ³]	Substrate material	Resonant frequency [GHz]	Return loss [dB]	Gain [dB]	Operating BW [GHz]	Relative BW %	
[1]	6.283x7.235x0.5	Roger RT Duroid 5880	27.854	-13.48	6.63	0.419	1.5	
[2]	85x8.5x0.244	FR-4	28	-40	7.58	1.064	3.74	
[3]	13.59x12x1.57	FR-4	28	-26	5.06	5.57	19.89	
[4]	10x8x1.57	FR-4	27	-40	6.6	4	9.14	
[5]	10.3x9x0.5	Roger RT duroid 5880	27.97	-20.95	7.5	1.06	29.9	
[6]	7.35x5.85x0.5	Roger RT duroid 5880	24-60	-12.63 to -46.23	Average 5.34	36	85	
[7]	7.56x6.57x0.5	RT Duroid 5880	26	-54.8	8	1.236	-	
[11]	15x15x0.508	Rogers RT5880	Single element	28.02	-30.02	6.639	2.305	8.19
				37.952	-20.15	8.578		
			Two elements	27.946	-27.84	7.581	3.651	6.09
				37.83	-18.35	9.24		
[12]	20x16x0.508	Rogers RT5880	25.98	-24.14	8.63	0.55	2.12	
			28.2	-25.43	11.26	1.1	3.93	
[13]	8.5x8x0.254	Rogers RT 5880	28	-32	6.7	-	-	
			38	-40	7.97	-	-	
[14]	8x8x1.6	FR-4	28	-15.88	7.18	15.7	48	
			38	-29.2	7.2	15.7	48	
[15]	6x7x0.5	Rogers RO3003	20.6	-23.7	3.75	1	8.3	
			29.6	-24.3	5.51	2.46		
[16]	11x8x0.5	Rogers RT/duroid 5880	28.3	-21	2.6	-	-	
			50.3	-31	2.6	-	-	
This work	6.2x8.4x1.57	Rogers RT5880	Single	26	-13.2	7.88	5.368	19.3
				28	-25.166	7.38		
	Nearby MIMO		26	-11.83	7.96	5.47	19.5	
			28	-23.92	7.48			
	Inverted MIMO		26	-12.4	8.15	5.35	19.13	
			28	-25.9	7.63			
	Mirrored MIMO		26	-13.96	7.12	6.35	23.36	
			28	-16.8	7.73			

It has been found that larger antennas often achieve higher gains, while the proposed designs maintain competitive gains (up to 8.16 dB in the inverted MIMO configuration) despite their compact dimensions ($6.2 \times 8.4 \times 1.57 \text{ mm}^3$ for the single antenna). This compactness is particularly advantageous for their integration into modern 5G devices, such as smartphones and IoT systems, which demand minimal physical footprints. The mirrored MIMO configuration achieves the widest bandwidth (6.35 GHz), indicating its suitability for broader applications. However, this comes at the cost of an increased substrate size ($14.4 \times 8.4 \times 1.57 \text{ mm}^3$). Conversely, the single antenna achieves a narrower bandwidth (5.368 GHz) but retains a highly compact form factor, showcasing a balance between bandwidth and size. Finally, the inverted MIMO configuration achieves the highest gain (8.16 dB) while maintaining a bandwidth (5.35 GHz) comparable to that of the single antenna. This configuration demonstrates that moderate trade-offs in bandwidth can result in significant gain enhancements, which are critical for improving signal strength and communication reliability in 5G systems. After a thorough comparison, it is observed that the single antenna and nearby MIMO configurations are ideal for devices with strict size constraints. The inverted MIMO configuration is well-suited for scenarios demanding enhanced signal strength, such as long-range or high-density urban environments. Furthermore, the mirrored MIMO configuration, with its broader bandwidth, is advantageous for multi-channel or wideband communication systems.

VI. CONCLUSIONS

This study designed and optimized a compact inset-feed microstrip antenna for fifth-generation (5G) applications, leveraging the Rogers RT5880 substrate. The antenna achieved operational resonant frequencies at 26 GHz and 28 GHz, with realized gains of 7.88 dB and 7.38 dB, respectively. Its operational bandwidth spans from 25.144 GHz to 30.512 GHz, yielding a bandwidth of 5.368 GHz and a relative bandwidth of 19.3%. The Half-Power Beam Width (HPBW) ranged from 82.3° to 90.9° , showcasing its directional characteristics. Further performance enhancements were achieved through three 2-by-1 MIMO configurations—nearby, inverted, and mirrored. The inverted MIMO configuration demonstrated the highest gains, reaching 8.16 dB at 26 GHz and 7.63 dB at 28 GHz, with an operational bandwidth of 5.35 GHz. The mirrored configuration provided the widest bandwidth at 6.35 GHz, indicating its potential for broader 5G applications. These results confirm the proposed design's capability to meet the high-performance demands of 5G communication systems, offering significant enhancements without increasing the transmitted power. This work contributes to the development of efficient and compact antenna systems for next-generation wireless technologies.

NOMENCLATURE

Symbol	Description
f_r	Resonant frequency (GHz)
λ	Wavelength (mm)
c	Speed of light in a vacuum (m/s)
ϵ_r	Relative permittivity of the substrate
h	Substrate height (mm)

W	Width of the patch (mm)
L	Length of the patch (mm)
Z_0	Characteristic impedance (Ω)
S_{11}	Reflection coefficient (dB)
S_{12}, S_{21}	Mutual coupling coefficients (dB)
BW	Bandwidth (GHz)
$HPBW$	Half Power Beam width (degrees)
G	Gain (dB)
$\tan\delta$	Loss tangent of the substrate
Γ	Reflection coefficient
Z_{in}	Input impedance (Ω)
R_{rad}	Radiation resistance (Ω)
h_s	Substrate height (mm)
t_p	Patch thickness (mm)
W_g	Width of the ground plane (mm)
L_g	Length of the ground plane (mm)
BW_r	Relative bandwidth (%)
μ	Efficiency %
x_0	Inset feed position (mm)
g	Inset feed gap (mm)
W_f	Feedline width (mm)
L_f	Feedline length (mm)
ΔL	Effective length extension due to fringing effects (mm)
L_{eff}	Effective length of the patch (mm)
k	Wave number ($2\pi/\lambda$)
ϑ	Azimuth angle (degrees)
θ	Elevation angle (degrees)
R	Distance from the antenna to observation point (m)
f_{gap}	Feed gap (mm)
ϵ_{eff}	Effective permittivity
W_p	Patch width (mm)
L_p	Patch length (mm)
t_g	Ground plane thickness (mm)

REFERENCES

- [1] O. Darboe, D. B. O. Konditi, and F. Manene, "A 28 GHz Rectangular Microstrip Patch Antenna for 5G Applications," *International Journal of Engineering Research and Technology*, vol. 12, no. 6, pp. 854–857, 2019.
- [2] M. T. Gameda, K. A. Fante, H. L. Goshu, and A. L. Goshu, "Design and Analysis of a 28 GHz Microstrip Patch Antenna for 5G Communication Systems," *International Research Journal of Engineering and Technology (IRJET)*, vol. 08, no. 02, pp. 882–886, Feb. 2021.
- [3] J. S. Alkasassbeh, F. M. Al-Taweel, T. A. Alawneh, A. Al-Qaisi, Y. F. Makableh, and T. El-Mezieni, "Advancements in Wireless Communication Technology: A Comprehensive Analysis of 4G to 7G Systems," *Journal of Wireless Mobile Networks, Ubiquitous Computing, and Dependable Applications*, vol. 15, no. 3, pp. 73–91, Sep. 2024, <https://doi.org/10.58346/IOWUA.2024.I3.006>.
- [4] R. Przesmycki, M. Bugaj, and L. Nowosielski, "Broadband Microstrip Antenna for 5G Wireless Systems Operating at 28 GHz," *Electronics*, vol. 10, no. 1, Jan. 2021, Art. no. 1, <https://doi.org/10.3390/electronics10010001>.
- [5] K. Kundu, A. Bhattacharya, F. H. Mohammed, and N. N. Pathak, "Design and Analysis of a Low-profile Microstrip Antenna for 5G Applications using AI-based PSO Approach," *Journal of Telecommunications and Information Technology*, no. 3, pp. 68–73, Sep. 2023, <https://doi.org/10.26636/jtit.2023.3.1368>.
- [6] S. E. Didi, I. Halkhams, M. Fattah, Y. Balboul, S. Mazer, and M. E. Bekkali, "Design of a microstrip antenna patch with a rectangular slot for 5G applications operating at 28 GHz," *TELKOMNIKA (Telecommunication Computing Electronics and Control)*, vol. 20, no. 3, pp. 527–536, Jun. 2022, <https://doi.org/10.12928/telkommika.v20i3.23159>.

- [7] D. A. Rahman, S. Y. Mohamad, N. A. Malek, D. A. Rahman, and S. N. Zabri, "A Wideband mm-Wave Printed Dipole Antenna for 5G Applications," *Indonesian Journal of Electrical Engineering and Computer Science*, vol. 10, no. 3, pp. 943–950, Jun. 2018, <https://doi.org/10.11591/ijeecs.v10.i3.pp943-950>.
- [8] P. R. Satarkar and R. B. Lohani, "Edge Port Excited Metamaterial Based Patch Antennas for 5G Application," *Communications and Network*, vol. 13, no. 3, pp. 111–129, Aug. 2021, <https://doi.org/10.4236/cn.2021.133009>.
- [9] A. S. Mohammed *et al.*, "A Review Of Microstrip Patch Antenna Design At 28 Ghz For 5G Applications System," *International Journal of Scientific & Technology Research*, vol. 8, no. 10, pp. 341–352, Oct. 2019.
- [10] N. Alaoui *et al.*, "Design of a microstrip antenna array for 5G applications," *International Conference on Frontiers in Academic Research*, vol. 1, pp. 334–338, Feb. 2023.
- [11] M. Li, "Broadband 5G Millimeter Wave Microstrip Antenna Design," *International Journal of Computer Applications Technology and Research*, vol. 8, no. 08, pp. 311–314, 2019.
- [12] H. M. Marzouk, A. Shaalan, and M. I. Ahmed, "A TWO-ELEMENT MICROSTRIP ANTENNA 28/38 GHZ FOR 5G MOBILE APPLICATIONS," *Delta University Scientific Journal*, vol. 3, no. 1, pp. 44–51, 2020.
- [13] M. Nahas, "A Super High Gain L-Slotted Microstrip Patch Antenna For 5G Mobile Systems Operating at 26 and 28 GHz," *Engineering, Technology & Applied Science Research*, vol. 12, no. 1, pp. 8053–8057, Feb. 2022, <https://doi.org/10.48084/etasr.4657>.
- [14] W. Hussain, M. I. Khattak, M. A. K. Khattak, and M. Anab, "Multiband Microstrip Patch Antenna for 5G Wireless Communication," *International Journal of Engineering Works*, vol. 07, no. 01, Jan. 2020, <https://doi.org/10.34259/ijew.20.7011521>.
- [15] S. S. Azizan, N. Al-Fadhali, and H. Majid, "Design A Wideband (25-40 GHz) Mm-Wave Microstrip Antenna for 5g Applications," *Progress in Engineering Application and Technology*, vol. 2, no. 2, pp. 609–620, 2021.
- [16] T. T. B. Ngoc, "Design of Microstrip Patch Antenna for 5g Wireless Communication Applications," *Journal of Science Technology and Food*, vol. 20, no. 2, pp. 53–61, 2020.
- [17] T. Kiran, N. Mounisha, C. Mythily, and D. Akhil, "Design of Microstrip Patch Antenna for 5g Applications," *IOSR Journal of Electronics and Communication Engineering*, vol. 13, no. 1, pp. 14–17, 2018, <https://doi.org/10.9790/2834-1301011417>.
- [18] M. O. Dwairi, M. S. Soliman, A. A. Alahmadi, I. I. M. A. Sulayman, and S. H. A. Almalki, "Design regular fractal slot-antennas for ultra-wideband applications," in *2017 Progress In Electromagnetics Research Symposium - Spring (PIERS)*, Feb. 2017, pp. 3875–3880, <https://doi.org/10.1109/PIERS.2017.8262435>.
- [19] M. O. Al-Dwairi, A. Y. Hendi, M. S. Soliman, and M. A. Nisirat, "Design of A Compact Ultra-Wideband Antenna for Super-Wideband Technology," in *2019 13th European Conference on Antennas and Propagation (EuCAP)*, Mar. 2019, pp. 1–4.
- [20] M. S. Soliman, M. O. Dwairi, and A. A. Alahmadi, "Design and performance analysis of an UWB patch antenna with enhanced bandwidth characteristics," in *12th European Conference on Antennas and Propagation (EuCAP 2018)*, Apr. 2018, pp. 1–4, <https://doi.org/10.1049/cp.2018.1039>.
- [21] A. Hindi, E. Ttrrad, and M. Dwairi, "A Compact 2 × 1 MIMO Microstrip Patch Antenna with Enhanced Gain for UWB Applications," in *2023 IEEE Jordan International Joint Conference on Electrical Engineering and Information Technology (JEEIT)*, Feb. 2023, pp. 255–258, <https://doi.org/10.1109/JEEIT58638.2023.10185806>.
- [22] M. O. Dwairi, M. S. Soliman, A. Y. Hendi, and Z. AL-Qadi, "The effect of changing the formation of multiple input multiple output antennas on the gain," *International Journal of Electrical and Computer Engineering (IJECE)*, vol. 13, no. 1, pp. 531–548, Feb. 2023, <https://doi.org/10.11591/ijece.v13i1.pp531-548>.
- [23] M. O. Dwairi, "Increasing Gain Evaluation of 2×1 and 2×2 MIMO Microstrip Antennas," *Engineering, Technology & Applied Science Research*, vol. 11, no. 5, pp. 7531–7535, Oct. 2021, <https://doi.org/10.48084/etasr.4305>.
- [24] A. Derneryd, "A theoretical investigation of the rectangular microstrip antenna element," *IEEE Transactions on Antennas and Propagation*, vol. 26, no. 4, pp. 532–535, Jul. 1978, <https://doi.org/10.1109/TAP.1978.1141890>.
- [25] M. Kara, "Closed-form expressions for the resonant frequency of rectangular microstrip antenna elements with thick substrates," *Microwave and Optical Technology Letters*, vol. 12, no. 3, pp. 131–136, 1996, [https://doi.org/10.1002/\(SICI\)1098-2760\(19960620\)12:3<131::AID-MOP4>3.0.CO;2-I](https://doi.org/10.1002/(SICI)1098-2760(19960620)12:3<131::AID-MOP4>3.0.CO;2-I).
- [26] A. S. Adewumi, V. James, I. A. Azeez, and G. Atilade Àlàgbé, "Design, Simulation and Performance Evaluation of Microstrip Patch Antenna Geometries at 6G Network Frequencies," in *2024 International Conference on Science, Engineering and Business for Driving Sustainable Development Goals (SEB4SDG)*, Apr. 2024, pp. 1–7, <https://doi.org/10.1109/SEB4SDG60871.2024.10629864>.
- [27] M. Dwairi, E. Dwairi, and S. Moqbel, "A MIMO 28.5 GHz H-shaped microstrip patch antenna for 5G applications," in *IEEE Conference on Advanced Topics on Measurement and Simulation*, Romania, Constanta, Dec. 2024.

AUTHORS PROFILE



Jawdat S. Alkasassbeh (Senior Member, IEEE) was born in Jordan in 1983. He received a B.Sc. degree in communications engineering from the Department of Electrical Engineering, Faculty of Engineering, Mutah University, Al-Karak, Jordan, in 2006, and a master's degree in communications engineering from the University of Jordan, Amman, Jordan, in 2011. He received a PhD degree from the School of Mechanical Engineering and Electronic Information, China University of Geosciences, Wuhan, China, in 2021. His current research interests include applications of evolutionary algorithms, applied AI, power reduction of mobile communication mechanisms, digital wireless communication systems, radio link design, image processing, UWB microstrip patch antennas, and dielectric resonant antennas. He can be contacted at: jawdat1983@bau.edu.jo.



Amjed Y. Hindi is an associate professor at Al-Balqa Applied University in Amman, Jordan's Faculty of Engineering Technology's Electrical Engineering department. His areas of research interest are signal and image processing, UWB microstrip patch antennas, dielectric resonant antennas, antenna measurement techniques, and optimization methods in antenna design. Dr. Hindi is an IEEE and AESS IEEE member. He can be contacted at amjadhindi@bau.edu.jo.



Issam Tread is an associate professor at Jadara University's Department of Electrical and Communication Engineering. He received his Ph.D. degree in electrical and communication engineering at the Odessa National Academy of Communication, Odessa, Ukraine, in 2003. His research interests include image processing, digital communication, and microstrip antenna design. Since 2000, he has been a part of the Jordan Engineers Association (JEA). He can be contacted at: itrrad@jadara.edu.jo.



Majed O. Dwairi (Member, IEEE) is a full professor at Al-Balqa Applied University in Amman, Jordan's Faculty of Engineering Technology's Electrical Engineering department. His areas of research interest are optical communication, wireless communication, signal and image processing, UWB microstrip patch antennas, dielectric resonant antennas, antenna measurement techniques, and optimization methods in

antenna design. Dr. Dwairi is an IEEE and AESS IEEE member. He can be contacted at: majeddw@bau.edu.jo



Elvira A. Dwairi is employed at the Electrical Engineering Department of the Faculty of Engineering Technology/Al-Balqa Applied University, Amman-Jordan. She received her Bachelor's Degree in communication from the Ukraine State Academy of Communication in Odessa. Her areas of research interest are microstrip antenna optimization and design. She can be contacted at: alveradw@bau.edu.jo.



Mahmoud Alja'fari is an accomplished communication engineer with extensive academic and administrative experience. He holds a Master's degree (2009) and a Bachelor's degree (2005) in Communication Engineering from Mutah University. His research interests focus on encoding systems, antenna design, and transmitting and receiving systems. Currently, Mahmoud serves as the Director of Career Development for Southern Region Colleges at Al-Balqa Applied University, Jordan, a role he has held since 2024. His expertise and dedication have significantly contributed to advancing both academic and professional development initiatives in his field. For inquiries, he can be reached at mzej@bau.edu.jo.